ELSEVIER

Contents lists available at ScienceDirect

# Materials Science & Engineering A

journal homepage: www.elsevier.com/locate/msea



# Production of nanograin microstructure in steel nanocomposite



Roohollah Jamaati <sup>a,b,\*</sup>, Mohammad Reza Toroghinejad <sup>c</sup>, Sajjad Amirkhanlou <sup>d</sup>, Hossein Edris <sup>c</sup>

- <sup>a</sup> Department of Mechanical Engineering, Babol Noshirvani University of Technology, Babol, Iran
- <sup>b</sup> Young Researchers and Elite Club, Ayatollah Amoli Branch, Islamic Azad University, Amol, Iran
- <sup>c</sup> Department of Materials Engineering, Isfahan University of Technology, Isfahan 84156-83111, Iran
- <sup>d</sup> Young Researchers and Elite Club, Najafabad Branch, Islamic Azad University, Najafabad, Iran

## ARTICLE INFO

#### Article history: Received 24 December 2014 Received in revised form 31 March 2015 Accepted 3 April 2015 Available online 14 April 2015

Keywords: Nanocomposites Nanostructured materials Accumulative roll bonding

#### ABSTRACT

In this study, microstructure and mechanical properties of steel/2 vol% SiC nanocomposite fabricated via accumulative roll bonding (ARB) process were investigated. Microstructure of nanocomposites was studied by scanning transmission electron microscopy (TEM). Tensile test also applied for determination of properties. In addition, the dislocation density was estimated from hardness measurement. The results indicated that continuously dynamic recrystallization (CDRX) and discontinuously dynamic recrystallization (DDRX) occurred in the microstructure of steel-based nanocomposite and the nanograins (55 nm) were obtained after the final cycle. With increasing the number of ARB cycles, the dislocation density of nanocomposite increased. In addition, after the first cycle, a significant increase observed in the yield strength, from 84 MPa to 689 MPa which is almost 8.2 times greater than that of the initial sample. After final cycle, the yield strength value increased to 1189 MPa. The yield strength improvement was mostly due to the grain refinement and dislocations and to a lesser extent to the load bearing effects of second phase (SiC nanoparticles) and precipitates. The contribution of each of these mechanisms was evaluated.

© 2015 Elsevier B.V. All rights reserved.

## 1. Introduction

In recent years, bulk metals with nano- (<100 nm) and ultrafine-grained (<1000 nm) structures have attracted considerable interest owing to their unique physical and mechanical properties [1–3]. Most techniques that are used for grain refinement employ severe plastic deformation (SPD) to induce a high dislocation density in the material, which is then converted to low- and high-angle grain boundaries (LAGBs and HAGBs) upon further processing [4–6]. Several SPD processing techniques are currently available but the following five processes have attracted the most attention: equal channel angular pressing (ECAP), high-pressure torsion (HPT), multiple forging (MF), repetitive corrugations and straightening (RCS), and accumulative roll bonding (ARB) [1–7].

The technique of ARB was introduced by Saito et al. [8,9], a process which was supposed to overcome the limitation of the ECAP, namely the low productivity. The greatest advantage of this method is that it makes use of a conventional rolling facility [7,10]. In this process, a metal sheet is rolled to one-half of the thickness,

and the rolled sheet is cut into two halves and then the two halves sheets are stacked together. The stacked sheets are then rolled again to one-half thickness. To achieve good bonding during the rolling operation, the two contact faces are degreased and wire brushed before placing them in contact. Therefore, a series of rolling, cutting, brushing, and stacking operations are repeated so that ultimately a large strain is accumulated in the sheet [11–16].

The effects of ARB process on microstructural evolution have been reported numerously for many materials including interstitial free (IF) steel [9,13,17-21]. So far, many efforts have been made to achieve nanostructure in the IF steel but had none of the researchers have managed to create a nanostructure in the IF steel. The minimum grain size of severe plastic deformation methods applied on the IF steel by different researchers was about 300 nm. Thus, the widespread use of the steel in various industries and the immense benefits of nanostructured materials mentioned at the beginning of the section and due to the failure to achieve nanostructured IF steel, the present researchers encouraged to take action in this area. But to achieve nanostructure in the IF steel by ARB process, what should we do? One of the strategies that can be effective is preventing the easy movement of dislocations and occurrence of recovery by second-phase particles. Recently, the present authors have been investigated the mechanical properties of IF steel/SiC nanocomposite fabricated by ARB process [22]. However, to the best of the authors' knowledge, no study in the

<sup>\*</sup> Corresponding author at: Department of Mechanical Engineering, Babol Noshirvani University of Technology, Babol, Iran. Tel.:  $+98\,911\,2124023$ .

E-mail addresses: jamaati@nit.ac.ir, r.jamaatikenari@ma.iut.ac.ir, roohollah144@gmail.com (R. Jamaati).

open literature reports on the microstructure evolution of the ARB-processed steel/SiC nanocomposite by scanning transmission electron microscopy (STEM). Thus, in the present study, the evolving microstructure of steel-based nanocomposite sheets during accumulative roll bonding has been investigated.

### 2. Experimental procedure

The materials used in this study were fully annealed sheets of interstitial free steel (specifications are given in Table 1) and SiC nanoparticles with size of 50 nm (Fig. 1). The microstructure of the IF steel is shown in Fig. 2. Four sheets of 150 mm  $\times$  50 mm  $\times$  0.7 mm were degreased via acetone and scratch brushed with a stainless steel wire brush 0.25 mm in diameter. After surface preparation, SiC nanoparticles were dispersed between the four sheets which were then stacked over each other and fastened at both ends by steel wires. To achieve a uniform dispersion of SiC nanoparticles between the IF steel sheets, an acetone-based suspension was prepared and ultrasonicated for 30 min. The suspension was sprayed on the sheets with a hand atomizer. Then, SiC nanoparticles were deposited and the acetone evaporated in air, so that the brushed surfaces of sheets were uniformly covered with SiC nanoparticles. The roll bonding process carried out at room temperature with no lubrication and using a laboratory rolling mill, with a loading capacity of 50 t. The roll diameter and the rolling speed were 220 mm and 6 m/min, respectively. The roll bonding process performed with an amount of thickness reduction equal to 75% corresponding to a von Mises equivalent strain  $e_{vM}$  of 1.6 per cycle (first step). Then, the roll bonded sheets were cut into four pieces. Then, to achieve a uniform distribution of SiC nanoparticles in the steel matrix, the above procedure was repeated again up to fourth cycle without adding reinforcement particles (second step). It should be noted that the final thickness of each cycle was 0.7 mm. The schematic illustration of the ARB process for fabrication of steel nanocomposite is shown in Fig. 3.

The samples for scanning electron microscopy (SEM) observations were cut from the sheets and this was mounted in bakelite. Then, the samples were polished using 80–4000 grit water-proof SiC paper. Finally, the polishing was finished on a cloth using alumina paste of 3  $\mu m$ . Scanning electron microscopy PHILIPS XL30 was used.

The microstructural observations were performed using scanning transmission electron microscopy (STEM). Thin foils were prepared with electropolishing conducted at  $-30\,^{\circ}\text{C}$  using 60 V in a 5% perchloric acid/95% methanol solution. Multiple disc samples with 3 mm diameter were separated from thin foils. Then, the discs were prepared using a low angle Ion Milling System from Fischione Model 1010 with 5 kV operating voltage, 5 mA current, 2.5 h time duration, and angle of  $10^{\circ}$  conducted at  $-40\,^{\circ}\text{C}$ . Hitachi S-4800 field emission scanning electron microscope was used.

Vickers microhardness was measured according to the ASTM E384-11e1 standard. The surfaces used for indentation testing were ground with SiC papers and polished with a sequence of alumina particles suspensions. Vickers indentation tests were performed using loads in the range 0.01–2 N.

The tensile test samples were machined from the ARB-processed sheets, according to the ASTM: E8M tensile sample, oriented along the rolling direction. The gauge width and length of the tensile test samples were 6 and 25 mm, respectively. The tensile tests were conducted at room temperature on a Hounsfield H50KS testing machine at an initial strain rate of  $1.67 \times 10^{-4} \, \mathrm{s}^{-1}$ .

#### 3. Results and discussion

As can be seen in SEM image (Fig. 2) the grain size of starting material is in the range of  $10{\text -}50\,\mu m$ . STEM micrographs from the

**Table 1** Chemical composition of IF steel (in wt%).

С	N	Si	Mn	Cu	Ni	Ti	Fe
0.002	0.004	0.01	0.14	0.01	0.018	0.055	Bal.

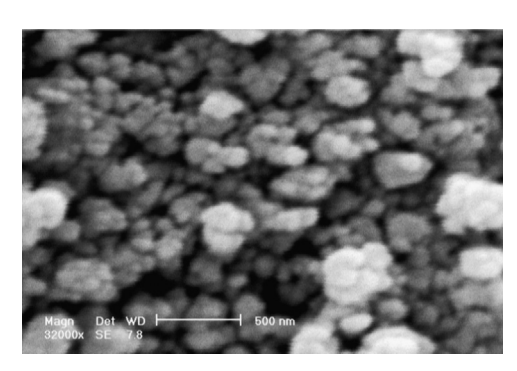
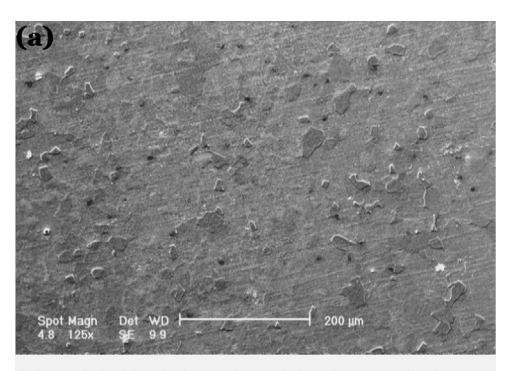


Fig. 1. SEM micrographs of the used SiC nanoparticles.



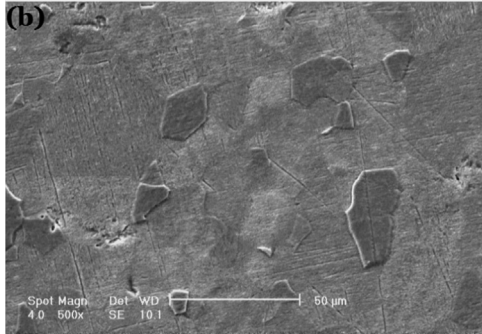


Fig. 2. Microstructure of the IF steel at two magnifications.

RD-TD plane of steel nanocomposite fabricated by ARB process after different cycles are shown in Fig. 4. Fig. 4(a) indicates that the sample contains grains with a size range from  $\sim\!25\,\text{nm}$  to 1.5  $\mu\text{m}$  and an average grain size of about 500 nm. The dislocation distribution seems completely nonuniform. In some areas, the individual dislocations and dislocation tangles were found frequently, and the dislocation density increased. On the other hand, in some areas dislocations are found both on the grain boundaries and inside the grains. Since dislocation contrast is visible within the grains and the grain boundaries are well defined, it is suggested that these nanoscaled grains are connected to discontinuous dynamic recrystallization (DDRX) and continuous dynamic recrystallization (CDRX) mechanisms. After two cycles of ARB process (Fig. 4(b)), the microstructure distribution is extremely nonuniform. Some areas show the nanograins microstructure (25-50 nm) which results from the CDRX and DDRX mechanisms. On the other hand, some areas demonstrate the micrograins microstructure (1  $\mu$ m). After third cycle, the fine grains

# Download English Version:

# https://daneshyari.com/en/article/7978009

Download Persian Version:

https://daneshyari.com/article/7978009

<u>Daneshyari.com</u>